

Received: 2016.10.11
Accepted: 2016.11.28
Published: 2017.07.07

Plasmid pLXSN-Mediated Adrenomedullin Gene Therapy for Cerebral Vasospasm Following Subarachnoid Hemorrhage in Rats

Authors' Contribution:
Study Design A
Data Collection B
Statistical Analysis C
Data Interpretation D
Manuscript Preparation E
Literature Search F
Funds Collection G

ABCD 1,2 **Xin Li**
DEFG 1 **Xiaoshuang Xia**
CDEFG 1 **Xin Li**

1 Department of Neurology, The Second Affiliated Hospital of Tianjin Medical University, Tianjin, P.R. China
2 1st Department of Neurology, The First Affiliated Hospital of Jiamusi University, Jiamusi, Heilongjiang, P.R. China

Corresponding Author: Xin Li, e-mail: lixinli@126.com
Source of support: Departmental sources

Background: The aim of this study was to investigate the protective effect of ADM gene mediated by plasmid pVAX1 on cerebral vasospasm (CVS) after subarachnoid hemorrhage (SAH).





Material/Methods: The recombinant plasmid pVAX-ADM was successfully established, and 40 SD rats were randomly divided into normal saline, pVAX1, pVAX1-ADM low-dose, pVAX1-ADM mid-dose, and pVAX1-ADM high-dose groups. The circumference and diameter of basilar artery, diameter of middle cerebral artery and internal carotid artery, and thickness of basilar artery wall were observed. The levels of circulating endothelial cells (CEC) and levels of regional cerebral blood flow (rCBF) of the parietal cortex were detected at different time-points. The expression levels of serum ADM, ET-1, and NOS of each group and the neurological functions were compared.

Results: The circumference and diameter of basilar artery and the diameter of the middle cerebral artery and internal carotid artery in pVAX1-ADM groups were significantly longer than those in the saline group and pVAX1 group ($P < 0.05$), but the thickness of the basilar artery wall in pVAX1-ADM groups was significantly lower ($P < 0.05$), and the levels of growth or decrease were both dose-dependent ($P < 0.05$). Compared with the saline group and pVAX1 group, the expression levels of serum ADM, NOS, and rCBF in pVAX1-ADM groups were significantly higher ($P < 0.05$), but the levels of serum ET-1 and CEC were significantly lower ($P < 0.05$). The scores of neurobehavioral functions of pVAX1-ADM groups were significantly lower ($P < 0.05$), and the scores were also dose-dependent ($P < 0.05$).

Conclusions: The recombinant eukaryotic expression plasmid pVAX1-ADM can significantly relieve cerebral vasospasm, increase the expression of serum ADM and NOS, and decrease the expression of serum ET-1 in a rat model of CVS; it is dose-dependent and can also improve nervous system function.

MeSH Keywords: **Adrenomedullin • Endothelin-1 • Nitric Oxide Synthase • Subarachnoid Hemorrhage • Vasospasm, Intracranial**

Full-text PDF: <http://www.medscimonit.com/abstract/index/idArt/901914>

 3749  5  7  27



Background

Subarachnoid hemorrhage (SAH) is a common type of hemorrhagic stroke, with high mortality and morbidity, and there is a trend of rising incidence rate in recent years [1]. Cerebral vasospasm (CVS) is an important complication after SAH; it occurs in 30% to 70% of SAH patients, and ischemic brain injury related to CVS is one of the major causes of death and disability [2,3]. It is believed that the oxidative stress, inflammatory reaction, apoptosis, and stimulation of toxic substances after SAH may be the pathogenic mechanism of CVS, but the exact mechanism remains unclear, so there is still no effective prevention strategy.

Adrenomedullin (ADM) is a polypeptide isolated from human pheochromocytoma by Japanese scholars in 1993. ADM is widely distributed in adrenaline, heart, lung, kidney, gastrointestinal tract, vascular endothelial cells, vascular smooth muscle cells (VSMC), myocardial cells, and other tissue cells. It has multiple biological effects, such as dilating blood vessels, inhibiting VSMC proliferation, stabilizing the internal environment, and regulating insulin levels, and is involved in embryonic growth, proliferation, and differentiation. It is also closely related with the occurrence and development of hypertension, coronary heart disease, heart failure, pulmonary hypertension, renal failure, endotoxin shock, and bronchial asthma [4,5]. ADM distributed in the brain can act as a neurotransmitter or neuromodulator, and is involved in the regulation of various physiological and pathological activities of the body. It is also involved in the regulation of cerebral circulation and the blood-brain barrier (BBB), has a strong relaxation effect on the blood vessels of brain, and has protective effects against ischemic and hemorrhagic cerebrovascular diseases [6].

So far, there is no report on the application of ADM in the treatment of cerebral vasospasm after subarachnoid hemorrhage. In the present study, we constructed a recombinant eukaryotic expression plasmid vector pVAX1-ADM that contained the ADM gene, by transferring the ADM gene into plasmid vector pVAX1 through genetic engineering. A rat model of cerebral vasospasm after subarachnoid hemorrhage was established with the Cisterna Magana blood injection method, and pVAX1-ADM was injected into the lateral ventricle by stereotactic technique. We observed the degree of basilar artery spasm and the expression of plasma endothelin-1, and explored whether plasmid pVAX1-ADM could prevent the reversal of cerebral vasospasm, as well as investigating the feasibility of plasmid-mediated ADM gene therapy for cerebral vasospasm after subarachnoid hemorrhage. This research could provide experimental evidence for the clinical treatment of cerebral vasospasm.

Material and Methods

Bacteria, vectors, and experimental reagents

The *Escherichia coli* strain JM109 was stored in the central laboratory. The cloning vector PMD-18T was purchased from Dalian Bao Bioengineering Co., Ltd.; the eukaryotic expression vector pVAX1 was purchased from Kebai Biotechnology Co., Ltd.; reverse transcription PCR (RT-PCR) and polymerase chain reaction (PCR) related reagents operating box were purchased from TAKARA Biotechnology Co., Ltd.; Markers, RNase inhibitors, HindIII Enzyme, Xba I enzyme, and T4 DNA ligase were purchased from Invitrogen Biotechnology Co., Limited; and the HE staining kit was purchased from Beijing Solaibao Technology Co., Ltd.

Construction, identification, and *in vitro* and *in vivo* expression of recombinant plasmid pVAX1-ADM

Total RNA extraction of rat adrenal tissue

Amplification of ADM gene by reverse transcription

(1) Upstream and downstream primer design of ADM gene:

The upstream and downstream primer sequences were as follows:

Upstream primer sequence: 5'-AAGCTTACCGCCATGTACCGCCAG-3'

Downstream primer sequence: 5'-TCTAGACTAATAGCCTTGAGGGTCTGATCTTG-3', the size of the amplified ADM gene sequence product was 174 bp.

(2) Specific steps of RT-PCR experiment:

RT-PCR reaction system:

| | |
|---|-------|
| 10×PCR buffer | 5 μl |
| MgCl ₂ (25 mmol/L) | 10 μl |
| dNTP mixture (10 mmol/L each) RNase Inhibiter (40 U/μl) | 5 μl |
| AMV RTase XL (5 U/μl) | 1 μl |
| AMV-Optimized Taq (5 U/μl) | 1 μl |
| ADM upstream primer (20 μmol/L) | 1 μl |
| ADM downstream primer (20 μmol/L) | 1 μl |
| Total RNA samples | 1 μl |
| RNase free H ₂ O | 4 μl |
| <hr/> | |
| Total | 30μl |

RT-PCR reaction conditions: 50°C (30 min)→94°C (5 min)→94°C (1 min)→55°C (30 s)→72°C (1 min), with a total of 25 cycles, and another 5 min of reaction at 72°C.

(3) Recycling and purification of amplified PCR product.

Connection and identification of T vector and AMD gene

Purity and concentration determination of recombinant plasmid

In vivo expression of recombinant plasmid pVAX1-ADM

We randomly 15 SD rats divided into 3 groups according to a digital table: the control group (n=5) received intramuscular injection of 1 ml saline in the left hind limb; the pVAX1 group (n=5) received intramuscular injection of 500 µg/kg pVAX1 solution; and the PVAX1-ADM group (n=5) received left hind limb intramuscular injection of 500 µg/kg pVAX1-ADM solution. All groups received 1 injection per week, for 4 continuous weeks. The expression of protein ADM in rat skeletal muscle was detected by immunohistochemistry.

Cell transfection with recombinant plasmid pVAX-ADM

293T cells were cultured in 10% FBS + DMEM medium and were transfected by pVAX1 or pVAX1-ADM with lipofectamine. The expression of protein ADM in the cells was detected by Western blot analysis at 48 h after transfection.

SAH animal modeling

SD rats were anesthetized with 10% chloral hydrate solution. The rats were fixed with stereotactic apparatus. The muscles and periosteum were separated one-by-one. The skull and atlas were completely exposed, and the incision was covered with sterile gauze. The rat tail was immersed in water at 60°C for 10 min, and was cut at the distance of 3–5 cm from the tail end, the 0.3 mL of blood was drawn. With the direction of the stereotactic apparatus, the needle was vertically inserted for about 1 mm to puncture the atlanto-occipital membrane, extracting 0.1 ml of cerebrospinal fluid. The tail blood was slowly injected into the occipital cistern with a micro-pump; the blood flow rate was at 0.1mL/min, and the puncture hole was sealed with bone wax. Finally, the muscles and skin were sutured. After the operation, the SD rats were kept in the prone position with the head down at a 30-degree angle for 0.5 h, which caused the blood to flow slowly into the base pool by the action of gravity.

Injection of plasmid

SD rats were fixed on the stereotactic apparatus and cut from the scalp to the skull along the sagittal line. The anterior fontanel was taken as the base point, moving backwards by 0.8 mm, then moved to the right by 1.5mm to drill the rat skull. Going 4.0 mm to 4.5 mm deeper with a micro-sampler, we then slowly injected 20 µl of normal saline in the saline group, 100 µg/kg

of pVAX1 in the pVAX1 group, 100 µg/kg of pVAX1-ADM in the low-pVAX1-ADM group, 500 µg/kg of pVAX1-ADM in the mid-pVAX1-ADM group, and 1000 µg/kg of pVAX1-ADM in the high-pVAX1-ADM group. The micro-sampler was removed 10 min after needle retention; we closed the surgical incision with bone wax, then sutured the muscles and skin, and finally disinfected the skin with iodine, after which rats resumed normal feeding.

Observation of the morphological changes of cerebral vasculature in SD rats

After 4 weeks of continuous injection of the plasmid, the morphological changes of cerebral blood vessels in SD rats were observed by HE staining. The circumference and diameter of basilar artery, diameter of middle cerebral artery and internal carotid artery, and thickness of basilar artery wall were observed and compared between groups.

Detection of circulating endothelial cells (CEC)

Detections were carried out before and after the modeling, and at 4 weeks after the injection of plasmid. We withdrew 0.5 ml of abdominal venous blood and added with 3.8% sodium citrate (0.5 ml) for anticoagulation, then we segregated, counted, SABC-FITC stained, and observed the sample with a laser scanning confocal microscope.

Detection of cerebral blood flow (rCBF) in the local parietal cortex

Detection was done at room temperature (26±2°C). In the resting state, rats were fixed in the prone position after anesthesia, and holes 2~3 mm in diameter were made 3 mm from the anterior fontanelle and the left side of the midline line, deep into the dura mater. A laser Doppler flowmeter probe was placed vertically in the dura mater and the position and depth of the probe were kept constant. The rCBF was measured before and after the modeling and at 4 weeks after the injection of plasmid. Cerebral blood flow signals were processed using LDF software, and the data were printed.

Statistical analysis

The data in this research were processed with SPSS13.0, measurement data are expressed as mean ± standard deviation, multi-group comparison was done with single-factor analysis of variance (one-way ANOVA), comparison between 2 groups was done with the LSD-T test, and P<0.05 indicates a statistically significant difference.

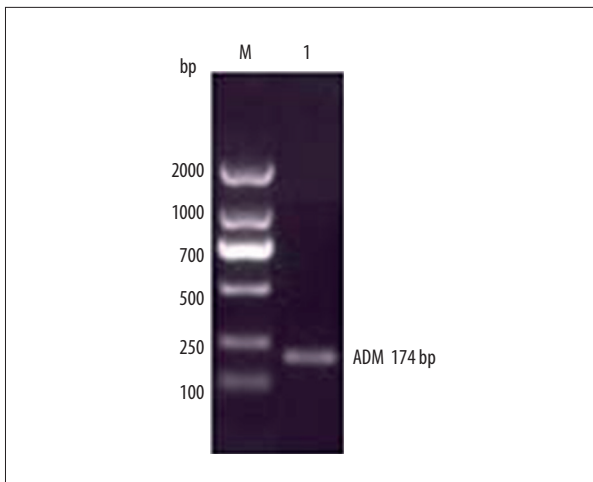


Figure 1. Results of RT-PCR electrophoresis of ADE gene.

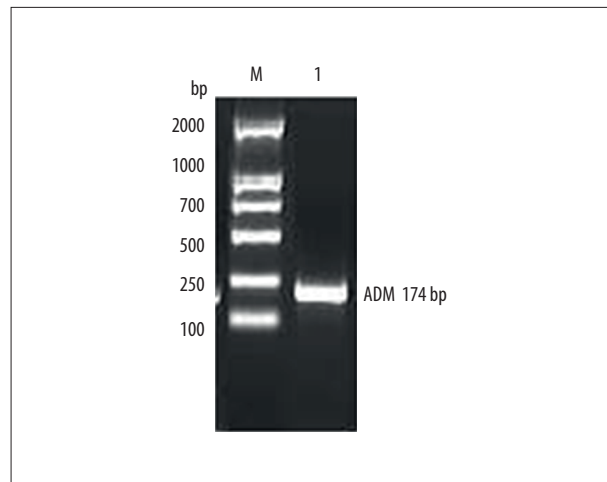


Figure 3. Identification of recombinant plasmid pVAX-ADM.

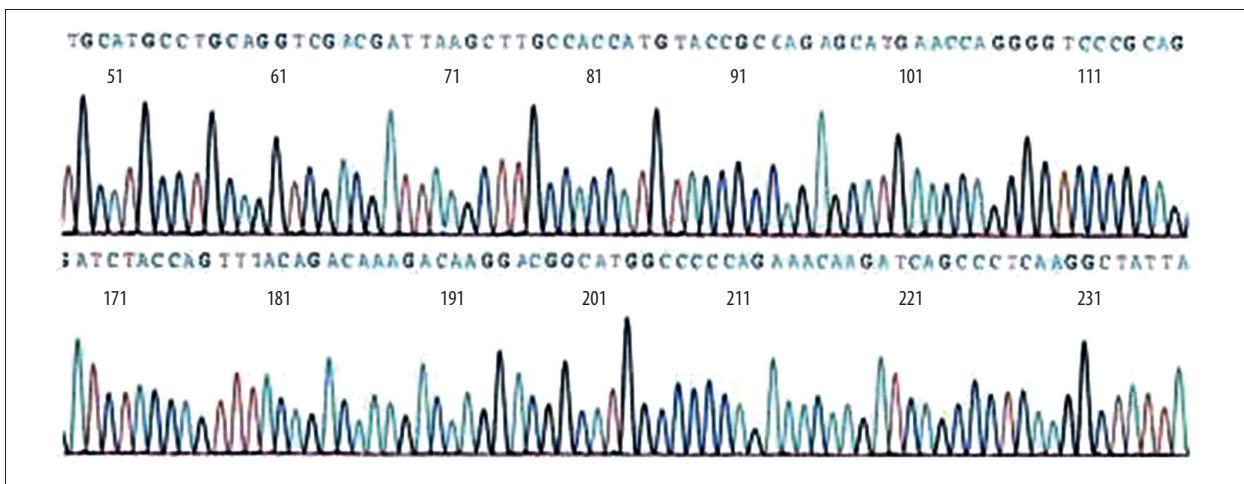


Figure 2. Sequencing identification of ADM gene.

Detection of serum ADM, ET-1, and NOS expression levels

After 4 weeks of continuous injection of plasmid, the expression levels of serum ADM was detected by ELISA, and the levels of serum ET-1 and NOS were detected by radioimmunoassay. The operation was performed strictly according to the instruction manual.

Scoring criteria of neurobiological function

After 4 weeks of continuous injection of plasmid, the neurological functions of SD rats in each group were evaluated according to the relevant diagnostic criteria, with a total possible score of 18 points, of which 1 point indicated an unstable experimental project or experimental reflex defects, 2 to 6 points indicated a mild injury of neurobiological function, 7 to 12 points indicated moderate neurobiological damage, and 13 to 18 points indicated severe neurological damage.

Results

Identification of ADM gene and recombinant plasmid pVAXI-ADM

The total RNA was extracted and ADM gene was amplified by RT-PCR. The results of RT-PCR amplification were analyzed in 2% gel electrophoresis, as shown in Figure 1, and ADM gene sequencing results are shown in Figure 2. The sequence of results was compared with that of the rat ADM gene in GeneBank. The 2 sequences were identical, suggesting that the ADM gene was needed for the experiment. PCR method was used to identify the recombinant plasmid pVAXI-ADM, and electrophoresis results are shown in Figure 3. The recombinant plasmid pVAXI-ADM was digested by double-enzyme digestion, the digested product was electrophoresed in 2% gel solution, and results are provided in Figure 4. Ultraviolet

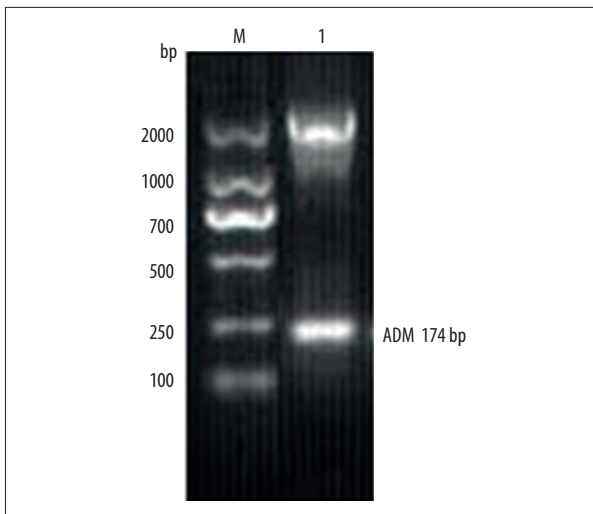
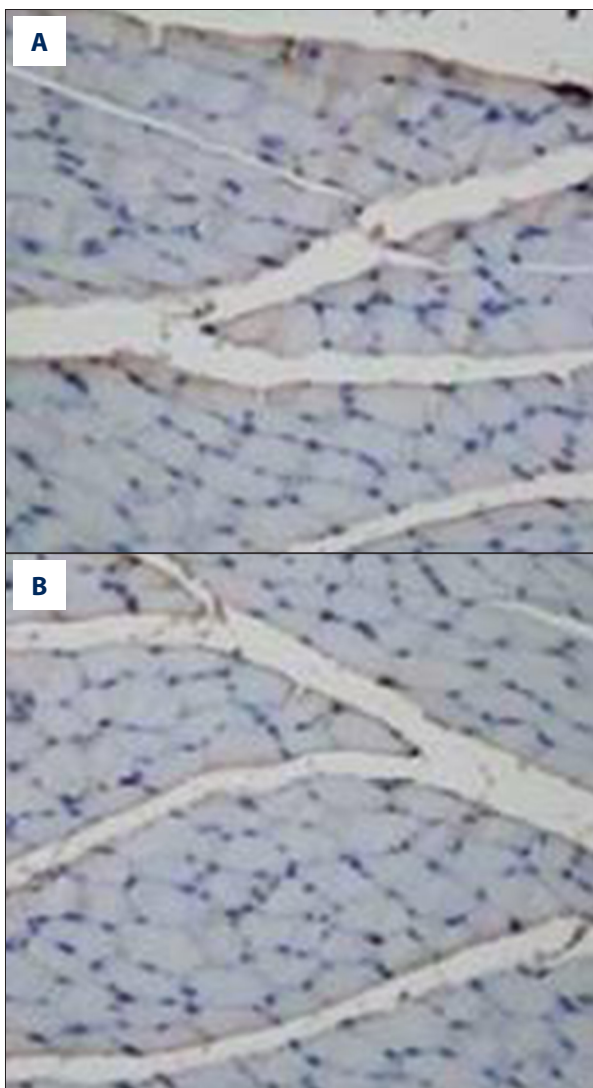


Figure 4. Identification of double-enzyme digested recombinant plasmid pVAX-ADM.



spectrophotometry was used for measurement of recombinant plasmid pVAX1-ADM, and $OD_{260}=0.917$, $OD_{260}/OD_{280}=1.812$, indicating the recombinant plasmid conformed to the purity requirement of this experiment. The concentration of recombinant plasmid pVAX1-ADM was estimated to be 4.59 mg/ml according to the formula.

The *in vitro* and *in vivo* expression of recombinant plasmid pVAX1-ADM

The expression of saline, pVAX1-blank plasmid, and pVAX1-ADM plasmid in rat gastrocnemius muscle tissue were detected, and positive expression was found in the pVAX1-ADM group, as shown in Figure 5A–5C. We separately transfected 4 μ g of pVAX1 plasmid and 4 μ g of pVAX1-ADM recombinant plasmid into 293T cells. Western blot analysis was then performed to measure the ADM protein expression, and ADM protein expression was discovered after pVAX1-ADM transfection, as shown in Figure 6.

Pathological examination of basilar artery in each group

The basilar arteries of each group were examined by light microscopy after HE staining. In the saline group and the pVAX1 group, the vascular wall was found to be significantly thickened, and the vascular lumen was narrowed. The endothelial cells were swollen and deformed. The inner elastic membrane became tortuous and wrinkled; it was dentate and intruded

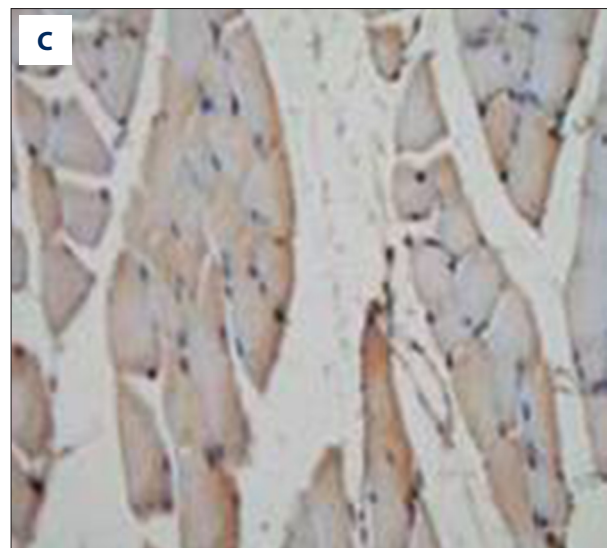


Figure 5. (A) Expression of saline in gastrocnemius tissue (immunohistochemical method $\times 200$). (B): Expression of pVAXI in gastrocnemius tissue (immunohistochemical method $\times 200$). (C) Expression of pVAXI-ADM in gastrocnemius tissue (immunohistochemical method $\times 200$). (A. pVAXI-ADM Group; B. pVAXI Group).

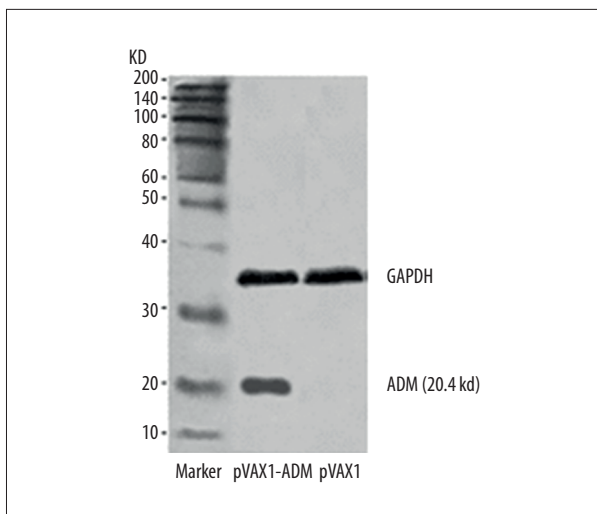
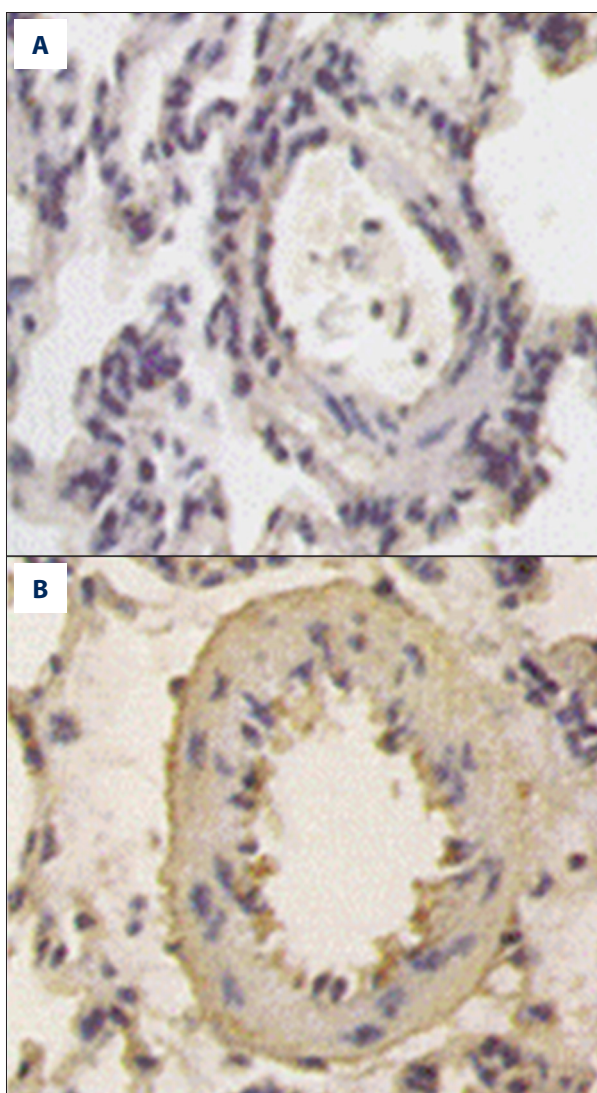


Figure 6. Expression of protein ADM in pVAX1-ADM after cell transfection.



into the vascular lumen. The intima-media thickened significantly, smooth muscle cell arrangement was chaotic, bending and deformation of nucleus were common, and vacuoles were occasionally found. The pathological changes of the basilar arteries in the pVAX1-ADM group were significantly improved compared with the saline group and the pVAX1 group (Figure 7A–7C).

Comparison of blood vessels in each group

The circumference and diameter of the basilar artery and the diameter of the middle cerebral artery and internal carotid artery of the pVAX1-ADM group (low-dose group, mid-dose group, high-dose group) were significantly greater than in the saline group and pVAX1 group ($P < 0.05$), but the thickness of the basilar artery wall was significantly lower than in the saline group and pVAX1 group ($P < 0.05$). With the increase of pVAX1-ADM injection dose, the circumference and diameter of the basilar artery and the diameter of the middle cerebral artery and internal carotid artery gradually increased ($P < 0.05$), and the thickness of the basilar artery wall decreased gradually ($P < 0.05$). However, no significant difference was found between the saline group and the pVAX1 group ($P > 0.05$), as shown in Table 1.

Comparison of the expression of serum ADM, ET-1, and NOS in each group

The expression of serum ADM and NOS in pVAX1-ADM groups (low-dose, mid-dose, high-dose) was significantly higher than

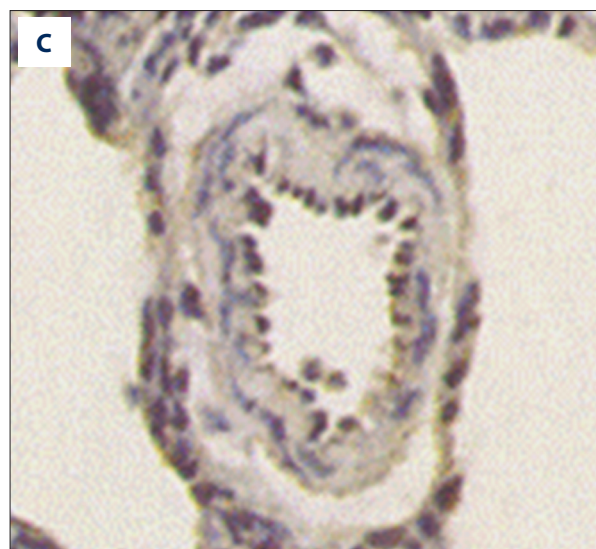


Figure 7. (A) Pathological manifestations of basilar artery of pVAX1-ADM group (HE staining $\times 200$). (B) Pathological manifestations of basilar artery of saline group (HE staining $\times 200$). (C) Pathological manifestations of basilar artery of pVAX1 group (HE staining $\times 200$).

Table 1. Comparison of blood vessels in each group.

| Groups | Cases | Circumference of basilar artery (μm) | Thickness of basilar artery wall (μm) | Diameter of basilar artery (μm) | Diameter of middle cerebral artery (μm) | Diameter of internal carotid artery (μm) |
|------------------------|-------|---|--|--|--|---|
| Saline | 8 | 457.22 \pm 57.81 | 24.67 \pm 2.74 | 227.76 \pm 10.23 | 168.27 \pm 8.76 | 230.52 \pm 9.84 |
| pVAX1 | 8 | 449.54 \pm 60.42 | 24.15 \pm 2.53 | 221.33 \pm 10.74 | 164.62 \pm 8.54 | 227.40 \pm 9.62 |
| pVAX1-ADM (low-dose) | 8 | 520.15 \pm 65.60* | 21.71 \pm 2.32* | 230.15 \pm 11.41* | 178.84 \pm 10.12* | 235.64 \pm 10.02* |
| pVAX1-ADM (mid-dose) | 8 | 577.81 \pm 72.32*# | 18.58 \pm 2.12*# | 242.81 \pm 12.55*# | 197.78 \pm 11.09*# | 244.85 \pm 11.21*# |
| pVAX1-ADMg (high-dose) | 8 | 632.87 \pm 80.15*#,@ | 16.47 \pm 1.82*#,@ | 257.65 \pm 14.05*#,@ | 215.43 \pm 12.14*#,@ | 253.61 \pm 12.45*#,@ |

Comparison with the saline group and pVAX group, * $P < 0.05$; comparison with the pVAX1-ADM low-dose group; # $P < 0.05$; comparison with the pVAX1-ADM mid-dose group, @ $P < 0.05$.

Table 2. Comparison of the expression of serum ADM, ET-1, and NOS expression in each group.

| Groups | Cases | ADM (ng/L) | ET-1 (ng/L) | NOS ($\times 10^3$ U/L) |
|------------------------|-------|------------------------|------------------------|--------------------------|
| Saline | 8 | 57.25 \pm 6.57 | 234.36 \pm 18.53 | 193.65 \pm 17.12 |
| pVAX1 | 8 | 56.94 \pm 6.93 | 229.87 \pm 18.53 | 191.27 \pm 17.63 |
| pVAX1-ADM (low-dose) | 8 | 78.43 \pm 8.92* | 198.62 \pm 17.02* | 207.42 \pm 15.74* |
| pVAX1-ADM (mid-dose) | 8 | 93.51 \pm 9.52*# | 162.44 \pm 16.72*# | 222.84 \pm 16.25**,# |
| pVAX1-ADMg (high-dose) | 8 | 108.45 \pm 11.46*#,@ | 141.38 \pm 14.52*#,@ | 239.95 \pm 18.05*#,@ |

Comparison with the saline group and pVAX group, * $P < 0.05$; comparison with the pVAX1-ADM low-dose group, # $P < 0.05$; comparison with the pVAX1-ADM mid-dose group, @ $P < 0.05$.

in the saline group and pVAX1 group ($P < 0.05$), and the expression of serum ET-1 was significantly higher than in the saline group and pVAX1 group ($P < 0.05$). With increased dose of pVAX1-ADM ($P < 0.05$), the level of serum ADM and NOS expression increased gradually ($P < 0.05$) and the level of serum ET-1 expression decreased gradually ($P < 0.05$). There was no significant difference between the saline group and the pVAX1 group ($P > 0.05$), as shown in Table 2.

Comparison of CEC levels at different time-points in each group

The differences in CEC levels between groups were found to be not significantly different either before or after the modeling ($P > 0.05$), but in all groups the CEC levels after the modeling were found to be significantly higher than those before the modeling ($P < 0.05$). The levels of CEC in the pVAX1-ADM group (low-, mid-, high-dose group) were significantly lower than those in the saline and pVAX1-ADM group ($P < 0.05$). With increased dose of pVAX1-ADM, the level of CEC decreased

gradually ($P < 0.05$), but no significant difference was found between the saline group and the pVAX1 group, as shown in Table 3.

Comparison of rCBF levels at different time-points in each group

The difference of rCBF levels between groups were found to be not significantly different either before or after the modeling ($P > 0.05$). In all groups, the rCBF levels after the modeling were found to be significantly lower than those before the modeling ($P < 0.05$). The levels of rCBF in the pVAX1-ADM group (low-, mid-, high-dose group) were significantly higher than those in the saline and pVAX1-ADM group ($P < 0.05$). With increased dose of pVAX1-ADM, the level of rCBF increased gradually ($P < 0.05$), but no significant difference was found between the saline group and the pVAX1 group ($P > 0.05$), as shown in Table 4.

Table 3. Between-group comparison of CEC levels at different time-points.

| Groups | Cases | Before modeling (1/0.9 µl) | After modeling (1/0.9 µl) | After 4 weeks of injection (1/0.9 µl) |
|------------------------|-------|----------------------------|---------------------------|---------------------------------------|
| Saline | 8 | 5.15±0.14 | 9.92±0.75 | 9.90±0.77 |
| pVAX1 | 8 | 5.14±0.13 | 9.95±0.74 | 9.94±0.73 |
| pVAX1-ADM (low-dose) | 8 | 5.13±0.15 | 9.91±0.77 | 8.42±0.54* |
| pVAX1-ADM (mid-dose) | 8 | 5.11±0.14 | 9.94±0.72 | 6.85±0.45*# |
| pVAX1-ADMg (high-dose) | 8 | 5.15±0.15 | 9.98±0.75 | 5.95±0.37*#,@ |

Comparison with the saline group and pVAX group, * $P<0.05$; comparison with the pVAX1-ADM low-dose group, # $P<0.05$; comparison with the pVAX1-ADM mid-dose group, @ $P<0.05$.

Table 4. Between-group comparison of rCBF levels at different time-points.

| Groups | Cases | Before modeling (PU) | After modeling (PU) | After 4 weeks of injection (PU) |
|------------------------|-------|----------------------|---------------------|---------------------------------|
| Saline | 8 | 616.54±14.12 | 243.84±24.74 | 244.62±25.16 |
| pVAX1 | 8 | 617.22±15.21 | 245.15±25.02 | 245.54±25.24 |
| pVAX1-ADM (low-dose) | 8 | 614.61±16.74 | 247.01±25.42 | 378.54±28.83* |
| pVAX1-ADM (mid-dose) | 8 | 615.91±16.30 | 246.14±25.25 | 491.26±30.55*# |
| pVAX1-ADMg (high-dose) | 8 | 619.04±17.11 | 248.07±25.64 | 582.43±31.64*#,@ |

Comparison with the saline group and pVAX group, * $P<0.05$; comparison with the pVAX1-ADM low-dose group, # $P<0.05$; comparison with the pVAX1-ADM mid-dose group, @ $P<0.05$.

Comparison of neurological function scores in each group

The neurological function scores of the pVAX1-ADM group (low-dose group, mid-dose group, and high-dose group) were significantly lower than those of the saline group and pVAX1 group ($P<0.05$). The neurological function scores decreased gradually with increasing dose of pVAX1-ADM ($P<0.05$). There was no significant difference between the saline group and the pVAX1 group ($P>0.05$). (Table 5).

Discussion

The main signaling pathway by which ADM exerts bioactivities is the association with its receptor, in which the N-terminal cyclic structure and C-terminal amide structure (16~52) are key receptor binding sites [7]. Specific ADM receptors are present in VSMC, endothelial cells, cerebral cortex, and cerebellar astrocytes. ADM can also play a vascular regulatory role when it binds to the calcitonin gene-related peptide receptor. When binding to receptors on vascular endothelial cells, ADM can increase the activity of inducible nitric oxide synthase in the cells, and promote the synthesis and release of nitric oxide, which

Table 5. Comparison of neurological function scores.

| Groups | Cases | Neurological function scores |
|------------------------|-------|------------------------------|
| Saline | 8 | 13.31±2.57 |
| pVAX1 | 8 | 13.24±2.63 |
| pVAX1-ADM (low-dose) | 8 | 11.32±2.43* |
| pVAX1-ADM (mid-dose) | 8 | 9.21±2.12*# |
| pVAX1-ADMg (high-dose) | 8 | 8.15±1.86*#,@ |

Comparison with the saline group and pVAX group, * $P<0.05$; comparison with the pVAX1-ADM low-dose group, # $P<0.05$; comparison with the pVAX1-ADM mid-dose group, @ $P<0.05$.

contributes to vasodilatation [8,9]. ADM can also inhibit the proliferation of VSMC and reduce atherosclerosis, by means of activating protein kinase A and inhibiting mitogen-activated protein kinase (MAPK) signal transduction pathways through the cAMP pathway after coupling with G protein [10,11]. Biological effects of ADM in the brain involve 3 different roles. The first role is regulation of the brain circulation: in the physiological

state, trace amounts of ADM in the plasma adjust the basilar vascular tension together with nitric oxide, prostacyclin, endothelin-1, and other vasoactive substances [12]. An experiment [13] confirmed that ADM in cerebral arteries of dogs and cats has a strong vasodilating effect, and it can regulate and maintain cerebral blood flow. The mechanism may be related to increased intracellular cAMP concentration and increased endothelial nitric oxide production [14]. The second role is BBB regulation: research [15] found that astrocyte secretion factor can induce cerebral vascular endothelial cells to generate ADM, participate in the differentiation and proliferation of vascular endothelial cells, and regulate BBB phenotype. ADM has a cAMP-like effect, it can reduce the permeability and phagocytosis of cerebral vascular endothelial cells and increase P-protein levels, playing an important role in accurate regulation of BBB through autocrine or paracrine [16]. The third role is stabilization of homeostasis: in the central nervous system, AM13-52, the ADM active fragment, can act on the adenohypophysis cells, inhibiting the secretion and release of adrenocorticotrophic hormone through the inhibition of basic and hormone-stimulating hormone in a dose-dependent manner [17]. It also works in the hypothalamus to reduce the secretion of vasopressin and aldosterone, so as to exert natriuretic effects, and regulates metabolism of water and salt and balance of electrolytes. In addition, ADM can inhibit basal and glucose-stimulated insulin secretion, but the lack of ADM can also damage the metabolism of carbohydrates and cause diabetes [18]. Therefore, a recombinant plasmid containing the ADM gene was constructed in this study; the construction was also confirmed successful by enzyme digestion, gene sequencing, and *in vitro* and *in vivo* experiments.

Early studies focused on the etiological relationship between ET-1 and CVS. Studies have shown that CVS increases cerebrospinal fluid and (or) peripheral blood ET-1 levels, and the selective ET_A receptor antagonist can significantly relieve CVS. ET-1 expression is upregulated during CVS development, and after SAH, cerebral blood vessels become even more sensitive to ET-1 [19–21]. Therefore, blood that comes from the ruptured cerebrovascular area and gets into the subarachnoid space and its metabolites is an important initiator of CVS. It can destroy the normal balance between vasoconstrictor factor ET-1 and nitric oxide (NO), and the imbalance leads to CVS after SAH [22]. However, the role of ET-1 in the pathophysiology of CVS remains unclear. Early studies have shown that, after SAH, ET-1 gets into the subarachnoid space and binds with vascular smooth muscle cell receptors, leading to the opening of non-selective calcium channels, influx of extracellular Ca²⁺, and results in contraction. Recent studies have shown that transient receptor potential (TRP) on smooth muscle cells may be associated with ET-1-induced CVS. *In vitro* experiments have shown that ET-1 (10 nmol/L) can induce the influx of extracellular Ca²⁺ in the basilar artery smooth muscle cells through

the non-selective calcium channels on the 4th and 7th day after SAH. The subtypes of TRP, TRPC1, TRPC4, or the heterodimer of both, play a more important role in the development of ET-1-induced CVS. Therefore, these subtypes may be a promising new target for the treatment of CVS after SAH [23]. Many animal experiments and clinical studies have shown that the increased ET-1 in cerebrospinal fluid may derive from the stimulation of neurons and astrocytes by subarachnoid blood and its metabolites, and the increased ET-1 in peripheral blood reflects the results of vascular endothelial dysfunction during SAH development. Cerebrospinal fluid and blood ET-1 may be involved in the occurrence and development of CVS, and ET-1 in cerebrospinal fluid may play a more important role [24]. In addition, in the occurrence and development of CVS, ET-1 receptor gets upregulated, and 5-HT and other spasmolytic factors also rise or its receptor gets upregulated; part of the spasm factor-specific inhibitor can also alleviate CVS symptoms to various degrees [25]. Thus, the mechanism of CVS includes multiple aspects such as the imbalance of lipid peroxides, endothelium-derived vasoconstrictor substances and vasodilating substances, metabolism of amino acid, inflammation, and endothelial cell proliferation, and necrosis may also participate in the occurrence and development of CVS; these spasm-initiation factors are interrelated, making it impossible to treat CVS through a single target [25].

NO is a micro-molecule with biological activity found in recent years. It plays an important role in regulating the cardiovascular system, nervous system, and immune function. NO is a direct vasodilator, which can diffuse rapidly into smooth muscle cells and cause vascular relaxation; therefore, it is an important factor in maintaining cerebrovascular tension. NO is generated by intracellular nitric oxide through catalyzing L-arginine with synthase. It acts as a mediator, messenger, or cell function regulator, and is involved in various physiological and pathological processes of the body. Decreased NO level is an important cause of CVS [26]. Nitric oxide in endothelial cells is catalyzed by synthase and releases NO, and NO rapidly enters the adjacent smooth muscle cells and activates soluble guanylyl cyclase, which generates cGMP when catalyzed. cGMP then activates the calcium pump in the intracellular sarcoplasmic reticulum, leading to the reduction of the intracellular free calcium, so that vascular smooth muscles become relaxed. Guanylate cyclase activity decreases when NO level is decreased; inadequate cGMP is generated, and the relaxation capacity of smooth muscles is reduced. Tiemey et al. [27] found that an NO release controller put around the blood vessels effectively inhibited vascular spasm caused by blood factors, which further confirms the role of NO in the pathogenesis of CVS.

Conclusions

The results of this study indicate that the circumference and diameter of the basilar artery, and the diameter of the middle cerebral artery and internal carotid artery in the pVAX1-ADM group were significantly longer than those in the saline group and pVAX1 group ($P < 0.05$), but the basilar artery wall thickness was significantly less than in the saline group and pVAX1 group ($P < 0.05$). With the increase of pVAX1-ADM injection dose, the circumference and diameter of the basilar artery and the diameter of the middle cerebral artery and internal carotid artery gradually increased ($P < 0.05$), and the thickness of the basilar artery wall decreased gradually ($P < 0.05$). The expression levels of serum ADM and NOS, and rCBF levels in the pVAX1-ADM group were significantly higher than those in the saline group and pVAX1 group ($P < 0.05$),

but the levels of serum ET-1 and CEC were significantly lower than that in the saline group and pVAX1 group ($P < 0.05$). The expression of serum ADM and NOS increased gradually with the increase of pVAX1-ADM injection dose ($P < 0.05$), and the expression of serum ET-1 decreased gradually. The scores of neurobehavioral functions of the pVAX1-ADM group were significantly lower than those of the saline group and pVAX1 group ($P < 0.05$); the scores also decreased gradually with the increase of pVAX1-ADM injection dose ($P < 0.05$). Therefore, it can be concluded that the recombinant eukaryotic expression plasmid pVAX1-ADM-carrying ADM gene can significantly relieve cerebral vasospasm, increase the expression levels of serum ADM and NOS, and decrease the expression of serum ET-1 in a rat model of CVS after SAH injection into the lateral ventricle. These effects are dose-dependent and improve nervous system function.

References:

- Danière F, Gascou G, Menjot de Champfleury N et al: Complications and follow up of subarachnoid hemorrhages. *Diagn Interv Imaging*, 2015; 96(7-8): 677-86
- Beck J, Raabe A: Clazosentan: Prevention of cerebral vasospasm and the potential to overcome infarction. *Acta Neurochir Suppl*, 2011; 110: 147-50
- Sharma BS, Sawarkar DP: Vasospasm: The enigma of subarachnoid hemorrhage. *Neurol India*, 2015; 63(4): 483-85
- Motokawa T, Miwa T, Mochizuki M: Adrenomedullin: A novel melanocyte dendrite branching factor. *J Dermatol Sci*, 2015; 79(3): 307-10
- Yuan M, Wang Q, Li C et al: Adrenomedullin in vascular endothelial injury and combination therapy: Time for a new paradigm. *Curr Vasc Pharmacol*, 2015; 13(4): 459-66
- Chen L, Yang X, Cui X et al: Adrenomedullin is a key protein mediating rotary cell culture system that induces the effects of simulated microgravity on human breast cancer cells. *Microgravity-Science and Technology*, 2015; 27(6): 417-26
- Pedreño M, Morell M, Robledo G et al: Adrenomedullin protects from experimental autoimmune encephalomyelitis at multiple levels. *Brain Beh Immun*, 2014; 37: 152-63
- Bigal ME, Walter S, Rapoport AM: Therapeutic antibodies against CGRP or its receptor. *Br J Clin Pharmacol*, 2015; 79(6): 886-95
- Akpinar A, Yaman GB, Demirdas A, Onal S: Possible role of adrenomedullin and nitric oxide in major depression. *Prog Neuropsychopharmacol Biol Psychiatry*, 2013; 46: 120-25
- Kitamura K: Reprint of "Adrenomedullin: A novel hypotensive peptide isolated from human pheochromocytoma". *Biochem Biophys Res Commun*, 2012; 425(3): 548-55
- Hussain QA, McKay IJ, Gonzales-Marin C, Allaker RP: Regulation of adrenomedullin and nitric oxide production by periodontal bacteria. *J Periodontol Res*, 2015; 50(5): 650-57
- Suzuki M, Asahara H, Endo S: Increased levels of nitrite/nitrate in the cerebrospinal fluid of patients with subarachnoid hemorrhage. *Neurosurg Rev*, 2009; 22(2-3): 96-98
- Nunobiki O, Nakamura M, Taniguchi E et al: Adrenomedullin, Bcl-2 and microvessel density in normal, hyperplastic and neoplastic endometrium. *Pathol Int*, 2009; 59(8): 530-36
- Kirisci M, Oktar GL, Ozogul C et al: Effects of adrenomedullin and vascular endothelial growth factor on ischemia/reperfusion injury in skeletal muscle in rats. *J Surg Res*, 2013; 185(1): 56-63
- Liverani E, Paul C: Glucocorticoids alter adrenomedullin receptor expression and secretion in endothelial-like cells and astrocytes. *Int J Biochem Cell Biol*, 2013; 45(12): 2715-23
- Endoh T1, Shibukawa Y, Tsumura M et al: Calcitonin gene-related peptide and adrenomedullin-induced facilitation of calcium current in submandibular ganglion. *Arch Oral Biol*, 2011; 56(2): 187-93
- Aggarwal G, Ramachandran V, Javeed N et al: Adrenomedullin is up-regulated in patients with pancreatic cancer and causes insulin resistance in β cells and mice. *Gastroenterology*, 2012; 143(6): 1510-17
- Zhou YB, Gao Q, Li P et al: Adrenomedullin attenuates vascular calcification in fructose-induced insulin resistance rats. *Acta Physiol (Oxf)*, 2013; 207(3): 437-46
- Kolias AG, Sen J, Belli A: Pathogenesis of cerebral vasospasm following aneurysmal subarachnoid hemorrhage: Putative mechanisms and novel approaches. *J Neurosci Res*, 2009; 87: 1-11
- Barth M, Capelle HH, Munch E et al: Effects of the selective endothelin A(ETA) receptor antagonist Clazosentan on cerebral perfusion and cerebral oxygenation following severe subarachnoid hemorrhage - preliminary results from a randomized clinical series. *Acta Neurochir (Wien)*, 2007; 149: 911-18
- Jorks D, Major S, Oliveira-Ferreira AI et al: Endothelin-1(1-31) induces spreading depolarization in rats. *Acta Neurochir Suppl*, 2011; 110: 111-17
- Miller AA, Budzyn K, Sobey CG: Vascular dysfunction in cerebrovascular disease: mechanisms and therapeutic intervention. *Clin Sci (Lond)*, 2010; 119: 1-17
- Xie A, Aihara Y, Bouryi VA et al: Novel mechanism of endothelin-1-induced vasospasm after subarachnoid hemorrhage. *J Cereb Blood Flow Metab*, 2007; 27: 1692-701
- Thampatty BP, Sherwood PR, Gallek MJ et al: Role of endothelin-1 in human aneurysmal subarachnoid hemorrhage: Associations with vasospasm and delayed cerebral ischemia. *Neurocrit Care*, 2011; 15: 19-27
- Edvinsson L, Povlsen GK: Late cerebral ischemia after subarachnoid haemorrhage: Is cerebrovascular receptor upregulation the mechanism behind? *Acta Physiol (Oxf)*, 2011; 203: 209-24
- Smith M, Citerio G: What's new in subarachnoid hemorrhage. *Intensive Care Med*, 2015; 41(1): 123-26
- Tiemey TS, Clatterbuck RE, Lawson C et al: Prevention and reversal of experimental posthemorrhagic vasospasm by the periaortic administration of nitric oxide from a controlled release polymer. *Neurosurgery*, 2006; 49(3): 945-51